Observed Trends in Various Aspects of Compound Heat Waves across China from 1961 to 2015

Yi LI[1,2,3*], Yihui DING[3], and Weijing LI[2,3]

1 *Chinese Academy of Meteorological Sciences*, *Beijing* 100081
2 *Collaborative Innovation Center on Forecast and Evaluation of Meteorological Disasters*, *Nanjing University of Information Science &Technology*, *Nanjing* 210044
3 *Laboratory for Climate Studies*, *National Climate Center*, *Beijing* 100081

(Received September 2, 2016; in final form November 8, 2016)

ABSTRACT

Based on combined thresholds of daily maximum and minimum temperatures, a compound heat wave is defined, and then changes in multiple aspects of such heat waves in China are estimated between 1961 and 2015. Our results intriguingly indicate that severe compound heat waves in northern China are characterized by excessively high intensity within short duration, while long duration determines great disaster-causing potential of severe events in the south. In the past few decades, large areas of China have experienced longer, stronger, and more frequent compound heat waves. Northern China has witnessed dramatic intensity increases, with a maximum amplification over 5°C decade^{-1}; while remarkable lengthening in duration has been mostly recorded in the south, with a maximum trend over 1 day decade^{-1}. The spatial extent affected by compound heat waves has significantly expanded since the 1960s, with the largest expanding rate over 6% decade^{-1} detected in North China and Northeast China. These systematic assessments serve to deepen our understanding of observed changes in compound heat waves across China, and may further shed some light on future adaptations and mitigations against an increasingly warming climate.

Key words: heat wave, climate change, duration, intensity, spatial extent

Citation: Li, Y., Y. H. Ding, and W. J. Li, 2017: Observed trends in various aspects of compound heat waves across China from 1961 to 2015. *J. Meteor. Res.*, **31**(3), 455–467, doi: 10.1007/s13351-017-6150-2.

1. Introduction

During summer, heat wave-induced morbidity and mortality among temperature-sensitive groups, like infants, the elderly, and cardiovascular patients, are alarmingly high. Such high impacts of heat waves have been reinforced by numerous literatures during the past few decades (Basu and Samet, 2002), and was punctuated by a record-breaking case in 2003, which hit vast areas of Europe and led to approximately 40000 deaths (García-Herrera et al., 2010). Furthermore, heat stress accumulated during heat waves could result in massive electricity shortages, higher risks of forest fire, and lower productivity of crops (García-Herrera et al., 2010). In general, heat waves (HWs) are commonly recognized as a spell of consecutive warm days, but concrete definitions differ among various sectors (Perkins et al., 2012). On a warming globe, increasing occurrences of warm days in many regions have elevated risks of heat waves (Stocker et al., 2013). In fact, most parts of the world have not only witnessed increased frequency, but also experienced higher intensity and longer duration of heat waves, especially after 2000 (Kuglitsch et al., 2010; Perkins et al., 2012; Smith et al., 2013). Increased frequency was largely ascribed to increased mean summertime temperature (Della-Marta et al., 2007), while amplified intensity resulted more from enhanced temperature variability (Fischer and Schär, 2010). Some climate model projections imply that these increases in mean and variability of summertime temperature will continue or even accele-

Supported by the National Basic Research and Development (973) Program of China (2013CB430203 and 2012CB417205), China Meteorological Administration Special Public Welfare Research Fund (GYHY201306033), National Natural Science Foundation of China (41275073), Program of Science and Technology Development in Sichuan Meteorological Bureau (2014-09), and Project for Postgraduate Scientific Research and Innovation of Jiangsu Province (KYLX16_0933).

*Corresponding author: liyiant@126.com.

rate, so more HWs with unprecedented duration and intensity will possibly happen by the end of the 21st century (Meehl and Tebaldi, 2004; Guo et al., 2017).

While one-day extremes of warm days/nights were widely investigated, comparably little work has been done to assess HWs comprehensively (Stocker et al., 2013), notably in China. In China, a finite number of studies concerned on definitions and changes of heat waves, in which consideration of HWs was mostly confined to high daytime heat (Jiang et al., 2012). However, long-lasting extreme weathers tend to trigger severer disasters, so indices measuring duration and intensity are also warranted (Zhang et al., 2011). It is now well-acknowledged that heat waves have significantly increased in China since the latter part of the 20th century (Ding et al., 2010; Ding and Qian, 2011; Wei and Chen, 2011; Wang et al., 2012). The frequency of hot weather events in Shanghai was much larger in the first decade of the 21st century than at any time since 1873 (Chen et al., 2013; Xia et al., 2016). In contrast, the scientific communities and governments in the US, Europe, and Australia are more concerned about compound heat waves composed of both warm days and nights, which may severely disturb human body thermoregulation and energy supply (Patz et al., 2005). Furthermore, in existing studies in China, changes in HW frequency seemed to be the primary concern, while other equally important indicators, such as duration, spatial coverage, and intensity, were substantially under-emphasized (Ding et al., 2010; Guo et al., 2017). In this context, a systematic estimation of compound HWs in China is still desirable. Our study therefore aims to narrow above-mentioned gaps of heat wave studies in China. Specifically, quantitative assessments would be performed with respect to changes of various aspects of compound HWs, including their frequency, number of days involved, duration, intensity, and spatial extent.

2. Data and methods

2.1 *Data*

Summertime (June–August) daily maximum temperature (T_{max}) and daily minimum temperature (T_{min}) between 1961 and 2015 are selected from a dataset covering 756 stations across China. This dataset is obtained from the National Meteorological Information Center (NMIC), China Meteorological Administration (CMA). Before being released, it has gone through fastidious quality control by the NMIC, with some missing observations completed, suspect/wrong values rectified, and temporal-spatial inconsistencies due to new instrumentations and site relocations reconciled (documentation available online at http://data.cma.cn/site/index.html). Having been validated in many studies (Chen and Zhai, 2013; Li et al., 2013; Ren and Zhou, 2014), this dataset is recognized as one of the best currently available for climate research in China. Apart from the above quality controls, we have performed some additional pretreatments to ensure that: 1) missing data for T_{max} and T_{min} account for less than 5% of total records in each year between 1961 and 2015; 2) any horizontal relocation of stations throughout the entire period is within a 20 km-radius; and 3) elevation relocation is less than 50 m vertically.

These procedures aim to guarantee the continuity and greatest homogeneity. This dataset covers almost all national reference climate stations (first-class stations) and national basic meteorological stations (second-class stations). The variables observed at each station represent the meteorological elements within a 20-km radius, so a relocation threshold of 20 km is routinely applied to minimize inhomogeneity from site displacements (Ren and Zhou, 2014). Particularly, site relocation doesn't mean significant changes in surface cover types, since environment (e.g., buildings and trees) in the vicinity of observational fields is universally stipulated by the CMA. A total of 376 stations are finally retained for subsequent analyses (see their distribution in Fig. 1), and these stations turn out well-distributed in eastern China, but sparsely scattered in western China.

2.2 *Methods*

Many studies defined heat waves based merely on T_{max} (Ding et al., 2010; Wang et al., 2012). In fact, consecutive hot days without relief from nighttime cooling are more devastating to human health (Karl and Knight, 1997; Meehl and Tebaldi, 2004). It is therefore necessary to define a heat wave with both the daytime high and overnight low being taken into account (Robinson, 2001). In this study, a heat wave is defined as a spell of three or more consecutive hot days and nights. Such a kind of heat wave is referred to as a "compound heat wave" hereafter. Three-day is adopted as a minimum duration to guarantee necessary persistency. Particularly, two independent heat waves are required to be sandwiched by at least two consecutive non-extreme day (T_{max} < 90th percentile or T_{min} < 90th percentile). A hot day/night is defined as one with a T_{max}/T_{min} above 90th percentiles of their respective long-term counterparts (1961–2015). Following the method introduced by Della-Marta et al. (2007), daily 90th percentile of T_{max}/T_{min} for each day during June–August is calculated from corres-

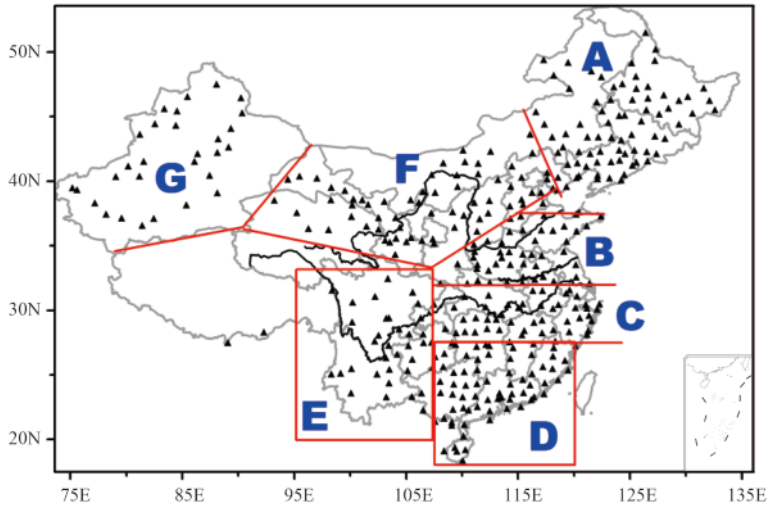

Fig. 1. Spatial distribution of 376 stations (marked by black triangles) under quality control procedure. Different regions are divided by red curves and labeled with blue letters: A for Northeast China, B for Huang-Huai, C for Yangtze River Valley, D for South China, E for Southwest China, F for North China, and G for Xinjiang.

ponding units of data samples, each of which contains 15 days (composed of the specific day and respective 7 days before and after it) in a given year; then these sample units for the days between 1961 and 2015 are assembled (i.e., total samples $15 \times 55 = 825$ days). A less critical threshold (90th percentile) for hot day/night is rationally adopted (Della-Marta et al., 2007), because an at-least 3-day duration and extreme T_{max}/T_{min} are required simultaneously. Identifications with higher percentiles (95th or 99th) substantially reduce the number of HWs, leading to many HW-undetected years (figure omitted). Few HW samples would impair the reliability of the following linear trend estimations. In existing studies, 90th percentile algorithm was also widely used to represent the rareness of temperature extremes (Fischer and Schär, 2010).

Figure 2 shows some illustrative examples depicting differences in identification based on daily percentiles and traditional seasonal percentiles. Daily 90th percentiles exhibit a pronounced intraseasonal variation, with lower thresholds in early and late summer, which is consistent with temporal evolution of observed T_{max}/T_{min}. Under a fixed seasonal percentile, early-summer (before 20 June) HWs are likely to be ignored (as shown in Figs. 2a, b), a problem prevailing over 90% of all stations. However, despite lower intensity, these early-summer HWs can be more health-damaging than mid-summer ones (Kalkstein and Smoyer, 1993). Early-summer HWs can trigger a greater death toll among susceptible populations who are overwhelmed by sudden scorching weather at so early stages (Kalkstein et al., 2008). By contrast, in mid to later summer, vulnerable groups may have become more adapted physiologically and behaviorally after long-time exposure to high ambient temperatures (Basu and Samet, 2002). During mid summer, similar HWs (Fig. 2b) can be identified by daily percentiles and seasonal thresholds at some stations. However, in many cases, the identified peak-summer HWs by seasonal percentiles fail to meet the daily percentile criteria, which tend to be more critical, as shown in Fig. 2c. In other words, in terms of intensity, daily percentiles may yield severer mid-summer HWs. The percentile-based threshold also enables HW changes comparable among regions of different prevailing climates (Robinson, 2001). Thus, the events identified by daily percentiles represent extremely hot anomalies, relative to normal conditions, from both temporal and spatial perspectives.

The definition doesn't entail an absolute threshold either (30°C or 35°C), as recommended by the CMA. In a warming climate, temperatures in some regions frequently exceeded these prescribed thresholds with no disastrous consequences to health or agriculture, thanks to technological (e.g., air conditioning and irrigation) or physiological precautions made in response to high temperature alerts. Based on varying daily percentiles, our HW definition, not only represents extremity statistically, but also emphasizes potential adverse impacts of these extremes (e.g., agricultural disasters, power outages, and water supply shortages) in the context of increasingly warming climate.

Four indices are designed to quantify heat waves: 1) heat wave number (HWN), that is, the occurrence times of heat wave events; 2) heat wave days (HWF), namely, the total number of days involved in all heat wave events; 3) heat wave duration (HWD), that is, the length

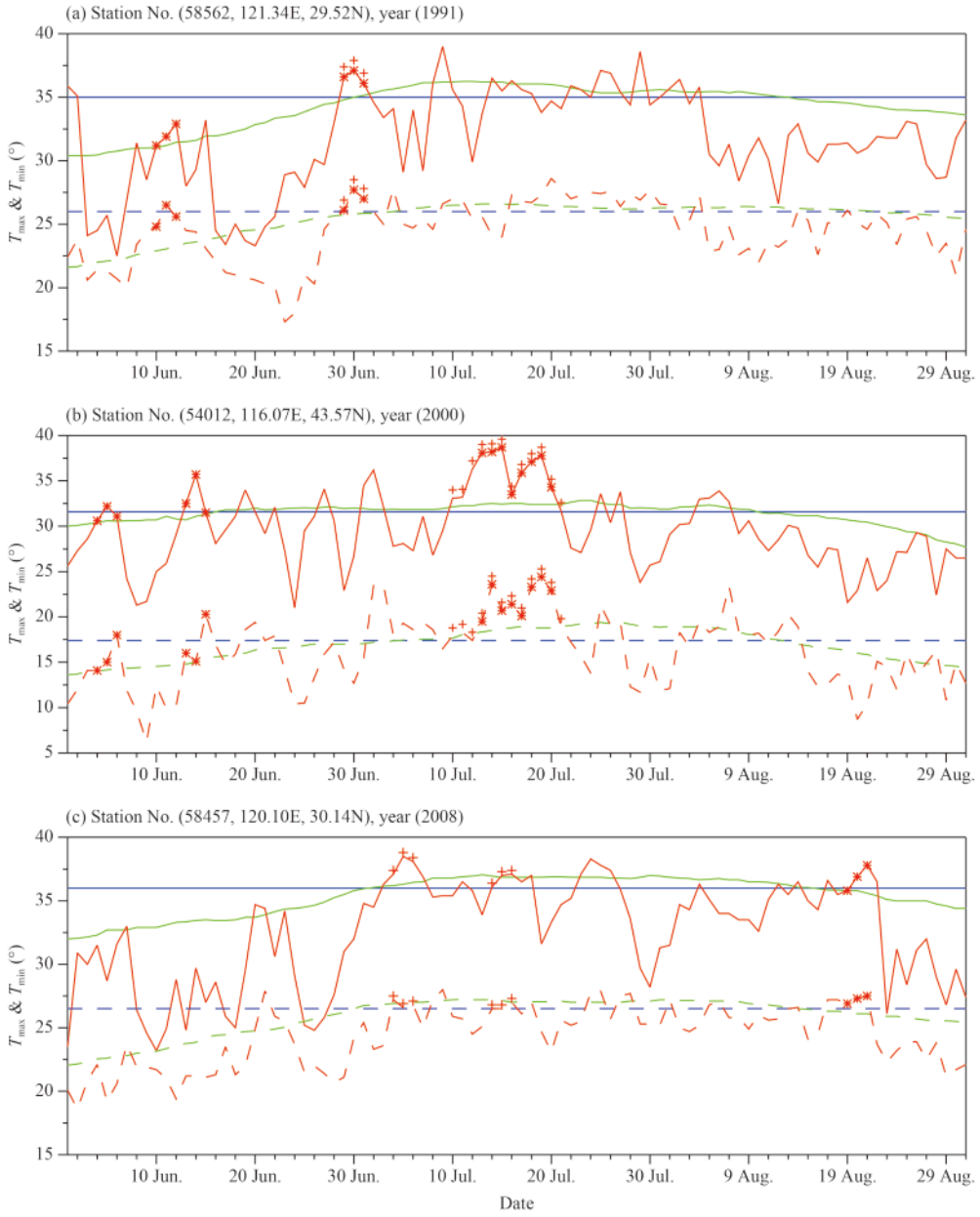

Fig. 2. Examples of heat wave identification by daily and seasonal thresholds. Solid blue (green) lines and dashed blue (green) lines represent seasonal (daily) 90th percentiles of T_{max} and T_{min} respectively; solid red lines and dashed red lines stand for T_{max} and T_{min} series; heat wave days identified by daily and seasonal 90th percentiles have been respectively labeled with "*" and "+".

of each heat wave; and 4) heat wave intensity (HWI), i.e., the amplitude of a heat wave calculated as accumulated exceedances of both T_{max} and T_{min} above certain thresholds during its duration, as follows,

$$\mathrm{HWI} = \sum_{t=1}^{\mathrm{Duration}} \left(T_{\max}(t) - T_{\max}\text{-threshold}(t)\right) + \left(T_{\min}(t) - T_{\min}\text{-threshold}(t)\right). \quad (1)$$

HWN considers the heat wave as a whole, while HWF tallies all extreme warm days/nights up during heat waves. For example, if there are 2 heat waves in a year, with one lasting for 3 days and the other for 5 days, then the annual HWN, HWF, and mean HWD are 2, 8, and 4 days, respectively. A great HWI, according to Eq. (1), may result from long duration and/or large exceedances above thresholds (Kuglitsch et al., 2010).

In addition to the above four indicators, an index measuring spatial extent of compound HWs is also constructed. To avoid possible uncertainties and inaccuracies brought in by interpolation, a method called "frozen grid" based on raw station observations, rather

than gridded data, is employed (Jones, 1986). Firstly, mainland China is divided into 2.5° longitude by 2.5° latitude boxes. Assuming there are totally ns(i) stations located within box-i, and among ns(i) stations, nh(i, t) stations record at least one heat wave during summer in year-t, the spatial coverage of HWs in year-t (for the whole country or a specific region) should be:

$$\text{Spatial\_coverage}(t) = \sum_{i=1}^{\text{number}} \frac{\text{nh}(i,t)}{\text{ns}(i)} \times 2.5 \times 2.5 \times 110 \times 110 \times \cos(\text{latitude}), \quad (2)$$

in which "110" denotes the approximate distance per unit longitude/latitude, and "number" represents the total number of boxes in the target region. Considering variation of box area with latitude, the spatial extent is also weighted by central latitude of each box. If simply represented by the number of affected stations, the spatial coverage in regions with sparse stations (e.g., Xinjiang and North China) would be much smaller than that in East China (an area boasting dense observational networks). Via the "frozen grid" scheme, the spatial coverage of compound HWs in different regions could be impartially compared by the percentages of stations recording HWs in boxes. The frozen grid method serves to minimize the influences of uneven station distribution on spatial extent evaluation (Chen and Zhai, 2013). Our sensitive tests indicate that selection of 2°, 2.5°, and 3° for the box scale significantly affects neither the estimated spatial coverage nor the following trend analyses. Considering varying box numbers among the sub-regions (see Section 3), in addition to absolute changes (km^2 decade^{-1}), the estimated spatial coverage of HWs is also normalized (divided) by respective total areas to yield percentages (% decade^{-1}) for convenience of further comparisons.

To evaluate linear trends of different parameters, Kendall's tau slope estimator (Sen, 1968) is employed. This nonparametric method is sufficiently insensitive to potential outliers, and it does not assume any distributional forms of the original data. Significance of linear trends at the 0.05 level is also estimated via the Kendall's tau test. The probability density function (PDF) is evaluated with kernel density estimation scheme, which is also detached from any prescribed assumption of distributional forms of the original data.

3. Results

3.1 *Basic features of HWs*

During the past 55 years, compound HWs occurred most frequently in the Yangtze River Valley (YRV) and South China (Fig. 3a), with a maximum accumulated occurrence of 80 recorded in Yin-Xian station in the YRV. Northern China also witnessed frequent HWs, with total occurrences of 30–40. During mid summer (21 June–10 August), daily 90th percentiles of $T_{\max}$ in central–eastern China, South China, and Northwest China usually exceed 35°C (Figs. 3b, 2a, 2c). Coincidently, daily 90th percentiles of $T_{\min}$ in these regions are higher than 20°C or even 25°C, meeting the "tropical nights" criterion ($T_{\min} \geqslant 20$°C, Fischer and Schär, 2010). Consistent with intraseasonal variations revealed in Fig. 2, daily percentiles in early summer (Fig. 3c) and late summer (Fig. 3d) are not as high as those in peak summer. During early summer, the configuration between extremely high daytime and nighttime percentiles mainly exist over northern parts of eastern China and Xinjiang area, while during late summer combined high percentiles mainly prevail in the south of the Huai River. Identified HWs based on such combined thresholds ($T_{\max} \geqslant 35$°C and $T_{\min} \geqslant 20$°C) reportedly account for excessive mortality (Grize et al., 2005). Remarkably, the adoption of daily percentiles explicitly accentuates regions with high risks of severe compound HWs during different summer stages.

Monthly distribution of HWs can also be obtained by utilizing daily percentiles (figure omitted). During June, HWs mainly hit the middle reach of the Yangtze River and coastal regions of South China. By contrast, July often witnesses HWs in the lower reaches of the Yangtze River, and northern and southern China. Long-lasting (over 5 days) HWs mainly concentrate during July, notably in mid–lower reaches of the Yangtze River. During August, the number of long-lasting HWs drops substantially, and high-frequency regions are distributed more dispersedly along the Yangtze River and southern coastal regions.

3.2 *Linear trend estimations*

Significant increases of nationwide HWN, HWF, HWD, and HWI (0.10 ± 0.04 decade^{-1}, 0.56 ± 0.20 days decade^{-1}, 0.10 ± 0.06 days decade^{-1}, and 0.75 ± 0.52°C decade^{-1}) are observed, which indicates more occurrences, longer duration, and greater intensity of HWs across China during the past few decades. Specifically, significant increases of HWN are mainly detected in northern (north of 35°N) and southern China (south of 30°N), sandwiched by a band of insignificant weak negative trends (Fig. 4a). The stations with a positive HWN trend of 0.4 decade^{-1} or greater are mainly located in the YRV and South China. The HWN has doubled in large swaths of China over the last decade, compared to that during the 1960s. The HWN in Southwest China has in-

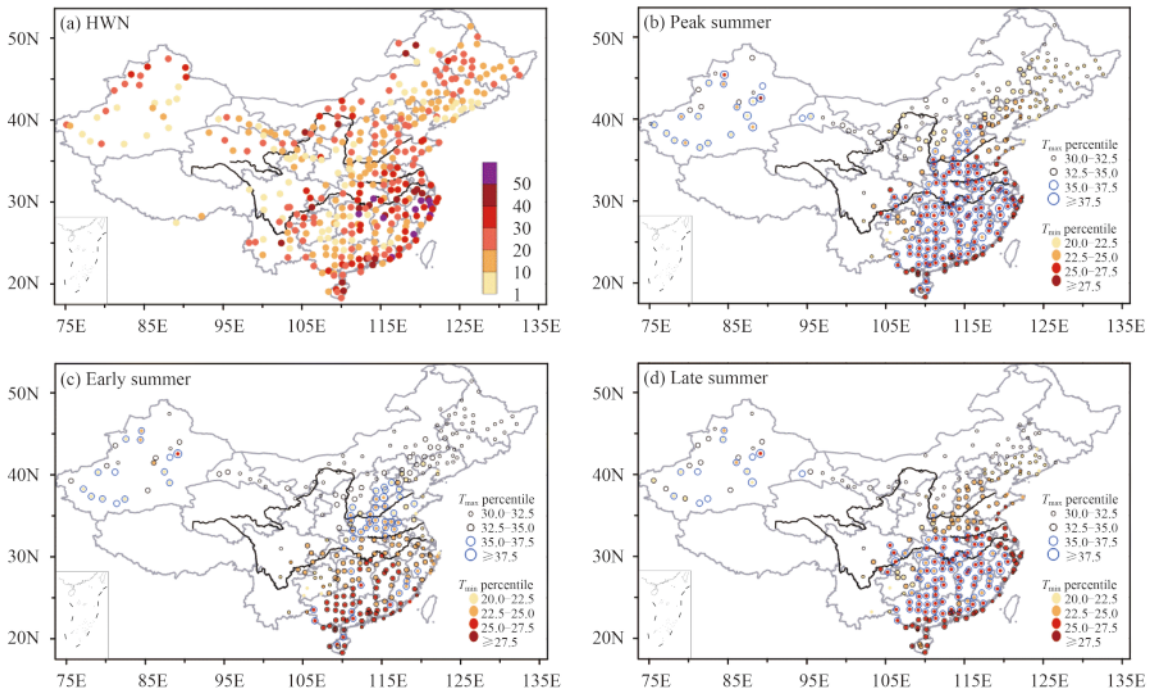

Fig. 3. (a) Total number of HWs (HWN) during 1961–2015. (b)–(d) Mean 90th percentiles of T_{max} and T_{min} in peak summer (21 June–10 August), early summer (1 June–20 June), and late summer (11 August–31 August), in which only stations with T_{max} (T_{min}) percentiles above 30°C (20°C) are presented.

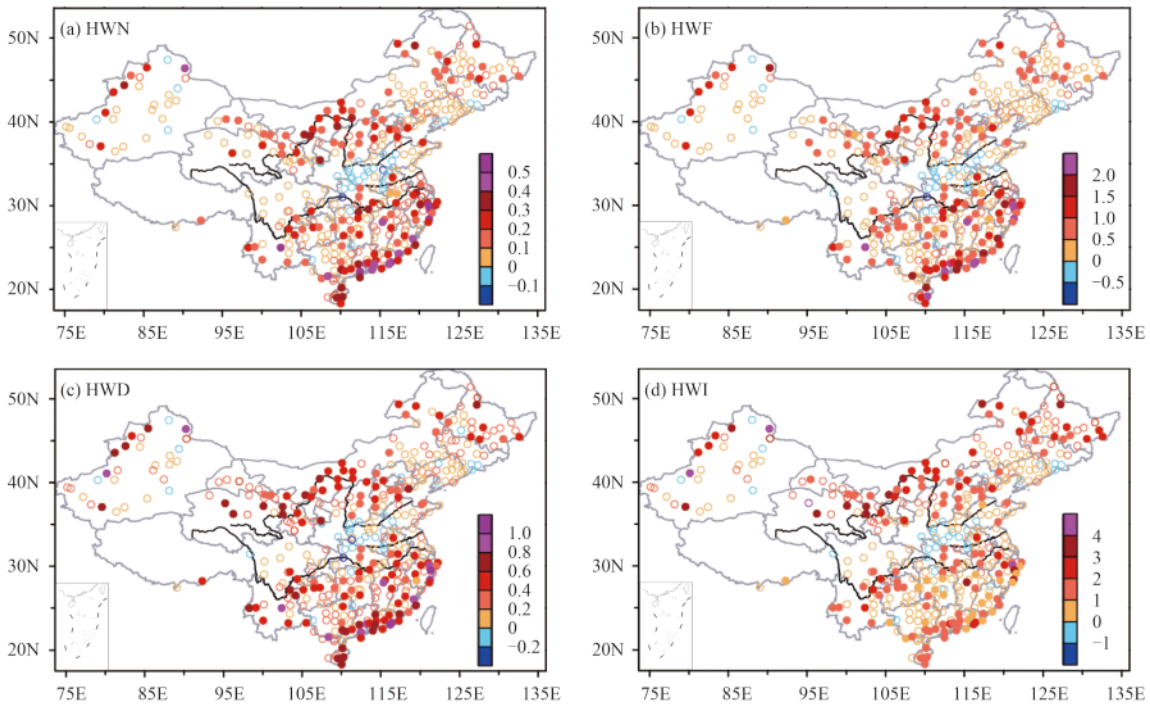

Fig. 4. Linear trends for (a) HWN (decade^{-1}), (b) HWF (days decade^{-1}), (c) mean HWD (days decade^{-1}), and (d) mean HWI (°C decade^{-1}). The filled dots indicate trends significant at the 0.05 level.

creased dramatically, from 0.60 per year in the 1960s to 1.53 per year in the last decade (figure omitted). Increasingly frequent HWs may partly account for severer droughts across Southwest China since 1995 (Wang et al., 2016). More heat wave days (i.e., higher HWF values) are also observed in most parts of China, which con-

stitutes a spatial pattern similar to that of HWN (Fig. 4b). The most significant increases in HWF are observed in the YRV and South China, with the largest linear trends above 3 days decade^{-1}. Compared to the 1960s, HWF in the YRV, Northeast China, and Southwest China has nearly tripled after 2000 (figure omitted). The mean duration of HWs in each year can be deduced via $\frac{\text{HWF}}{\text{HWN}}$, in which both indices have increased over most stations as discussed above. The lengthened duration in Fig. 4c suggests greater magnitude of growth in HWF than in HWN, and also implies an amalgamating trend between increasing warm days and nights. Mean HWI increases of 3°C decade^{-1} or above are mainly detected in northern China (Fig. 4d). Also greatly amplified (above 4°C decade^{-1}) is the mean intensity of HWs in the Yangtze River Delta dotted with several fast-developing metropolises, such as Shanghai. Trends for HWI in this densely-populated area are 2–3 times larger than those in the neighboring regions, implying possible anthropogenic contributions to heat wave intensification there. Representing accumulated exceedances above certain thresholds during HWs, HWI is determined by both duration and intensity of T_{max} and T_{min}. The magnitudes of duration increases in northern and southern China are similar (Fig. 4c), so much sharper increases of HWI in northern China arise more from greater growth in daily maximum and minimum temperatures at higher latitudes (Serreze et al., 2000). Frequent HWs with greater HWI have accelerated desertification and grassland degradation in Northern China, posing a great threat to local ecosystem and economy (Xue, 1996).

Remarkably, in contrast to significant positive trends in above regions, insignificant negative and weak trends of all HW indices are observed in regions between the Yellow River and the Yangtze River, which mainly result from significant decreases in hot days (Fig. 5a). Also revealed by Ding et al. (2010) and Ye et al. (2013), such drastic reductions in hot days have led to significant decreases in T_{max}-based heat waves in this area. Apparent differences in magnitude, significance, and even signs (positive/negative) of linear trends for compound HWs and T_{max}-based HWs further justify the necessity of separately assessing diverse heat wave types. A pan-China pattern of significant increases of hot nights (Fig. 5b) indicates a more sensitive response of nighttime low to climate warming, which may arise from natural variability and/or anthropogenic influences.

As shown in Fig. 4, trends for heat wave indices display distinctive regional peculiarities, matching well with climate zones classified by summer temperature (Zou et al., 2005; Liu and Zhai, 2014). Based on a comprehensive consideration of regional features of HW indices and climate zones, China is then divided into seven sub-regions as shown in Fig. 1. All the indices are then evaluated at regional scales as presented in Table 1. In general, greater increases of HWN, HWF, and mean HWD are found in South China, Southwest China, and the YRV. The largest increases of both HWN and HWF are observed in the YRV with respective linear trends of 0.24 ± 0.10 decade^{-1} and 1.13 ± 0.52 days decade^{-1}. The most obvious lengthening in duration is registered in Southwest China with a linear trend of 0.49 ± 0.18 days decade^{-1}. Larger increases in HWI are detected in northern China. In the Huang–Huai region, changes for all four indices are weak and insignificant.

The spatial extent of HW has increased nationwide at a linear trend of (41.16 ± 12.66) × 10^4 km^2 decade^{-1}. From another perspective, such an increasing trend can be translated into that compound HWs swept larger portions (4.43% ± 1.36% decade^{-1}) of mainland China, where few events of this type were registered in the past. Such a heat wave expansion is also manifested in each sub-region, as shown in Table 1. The maximum expansion of spatial coverage is detected in Northeast China

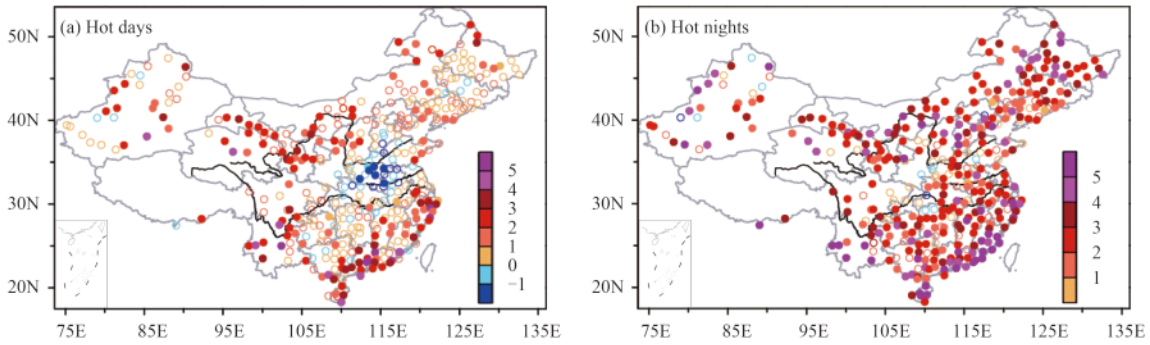

Fig. 5. Linear trends for occurrences of (a) hot days (days decade^{-1}) and (b) hot nights (days decade^{-1}). The filled circles indicate trends significant at the 0.05 level.

Table 1. Linear trends for domain-averaged HWN (decade^{-1}), HWF (days decade^{-1}), mean HWD (days decade^{-1}), mean HWI (°C decade^{-1}), and spatial extent (10^4 km^2 decade^{-1}, % decade^{-1} for the values in bracket) for the 7 sub-regions during 1961–2015

	YRV	South China	Xinjiang	North China	Northeast China	Huang–Huai	Southwest China
HWN	**0.24 ± 0.10**	**0.19 ± 0.06**	**0.16 ± 0.07**	**0.12 ± 0.08**	**0.14 ± 0.08**	–0.01 ± 0.92	**0.19 ± 0.06**
HWF	**1.13 ± 0.52**	**0.93 ± 0.29**	**0.74 ± 0.29**	**0.58 ± 0.34**	**0.56 ± 0.30**	–0.06 ± 0.37	**0.89 ± 0.26**
HWD	**0.32 ± 0.23**	**0.21 ± 0.13**	**0.42 ± 0.19**	0.18 ± 0.21	**0.28 ± 0.22**	–0.06 ± 0.24	**0.49 ± 0.18**
HWI	**1.24 ± 0.69**	**0.80 ± 0.35**	**2.01 ± 0.81**	**1.28 ± 1.01**	**1.81 ± 1.18**	0.43 ± 0.88	**1.78 ± 0.69**
Extent	**3.71 ± 2.52**	**4.79 ± 1.89**	**3.99 ± 1.69**	**9.12 ± 4.29**	**4.48 ± 1.15**	**3.71 ± 2.95**	**3.99 ± 1.57**
	(5.92 ± 4.02)	**(3.44 ± 1.35)**	**(4.44 ± 1.88)**	**(6.40 ± 3.01)**	**(6.73 ± 1.73)**	**(3.38 ± 2.69)**	**(3.96 ± 1.56)**

Note: Trends in bold indicate a significance level of 0.05. The error estimates are at 95% confidence intervals based on the standard error of the Kendall's tau estimator. The linear trends of the "Extent Index" are further normalized (divided) by respective total areas of each sub-region, as listed in the second row of "Extent".

and North China, with about extra 6% intact territory in these regions scorched by compound HWs per decade after 1961. Of particular note is that despite no significant increases or even slight decreases in occurrences of compound HWs in the Huang–Huai region, spatial coverage exhibits a significant positive trend there. This implies that compound HWs tend to appear more evenly across the Huang–Huai region, rather than to repeatedly occur at some specific stations. Multi-model projections of HW coverage imply that the regions suffering compound HWs would further expand (Guo et al., 2017).

3.3 *Severe HWs*

Severe heat waves, characterized by long duration and/or high intensity, would result in serious casualty and economic damage. D'Ippoliti et al. (2010) concluded that in some European cities, the mortality was up to 3 times greater during severe HWs than moderate HWs. To further assess severe HWs, linear trends for the annual longest duration and maximum intensity of HWs are explored (as displayed in Fig. 6). Sharpest lengthening of the longest duration has occurred in the YRV and South China, while the largest increase of maximum intensity (above 3°C decade^{-1}) is observed in North China. The T_{max} and T_{min} in most days during strongest HWs exceed their 95th or even 99th percentile, although they are originally identified based on their respective 90th percentile. Within each sub-region, the events with the longest duration and maximum intensity are selected among all stations to intuitively demonstrate the severity of these high-impact HWs (Fig. 7). The lengthening trend of the longest duration and increases of the maximum intensity are clearly revealed in Fig. 7 and validated in Table 2. Figure 7 shows a general consistency between durations of the strongest HWs (dashed lines) and the longest-lasting events (red bars), which highlights long duration's role in extraordinary heat stress accumulation. In the YRV and southern China, the longest duration usually exceeds a week. A typical case is that a 22-day compound HW affected South China in 1998. In such long-lasting heat waves, duration plays a more critical role than intensity in elevating mortality. Mortality grows

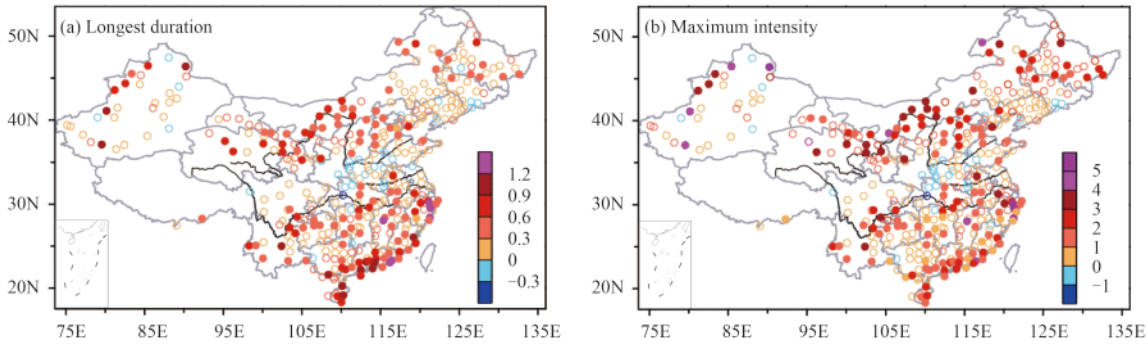

Fig. 6. Linear trends for (a) longest duration (days decade^{-1}), (b) maximum intensity (°C decade^{-1}) at each station. The filled circles indicate trends significant at the 0.05 level.

Table 2. Linear trends for longest duration (days decade^{-1}), and maximum intensity (°C decade^{-1}) for the 7 in sub-regions during 1961–2015

	YRV	South China	Xinjiang	North China	Northeast China	Huang–Huai	Southwest China
Longest duration	**1.11 ± 0.80**	**1.47 ± 0.50**	**0.93 ± 0.28**	**0.89 ± 0.43**	**0.63 ± 0.36**	–0.04 ± 0.46	**1.17 ± 0.31**
Maximum intensity	**6.10 ± 3.32**	**4.71 ± 1.33**	**4.99 ± 2.07**	**5.25 ± 3.22**	**4.81 ± 2.44**	1.80 ± 2.32	**4.77 ± 1.59**

Note: Trends in bold indicate a significance level of 0.05. The error estimates are at 95% confidence intervals based on the standard error of the Kendall's tau estimator.

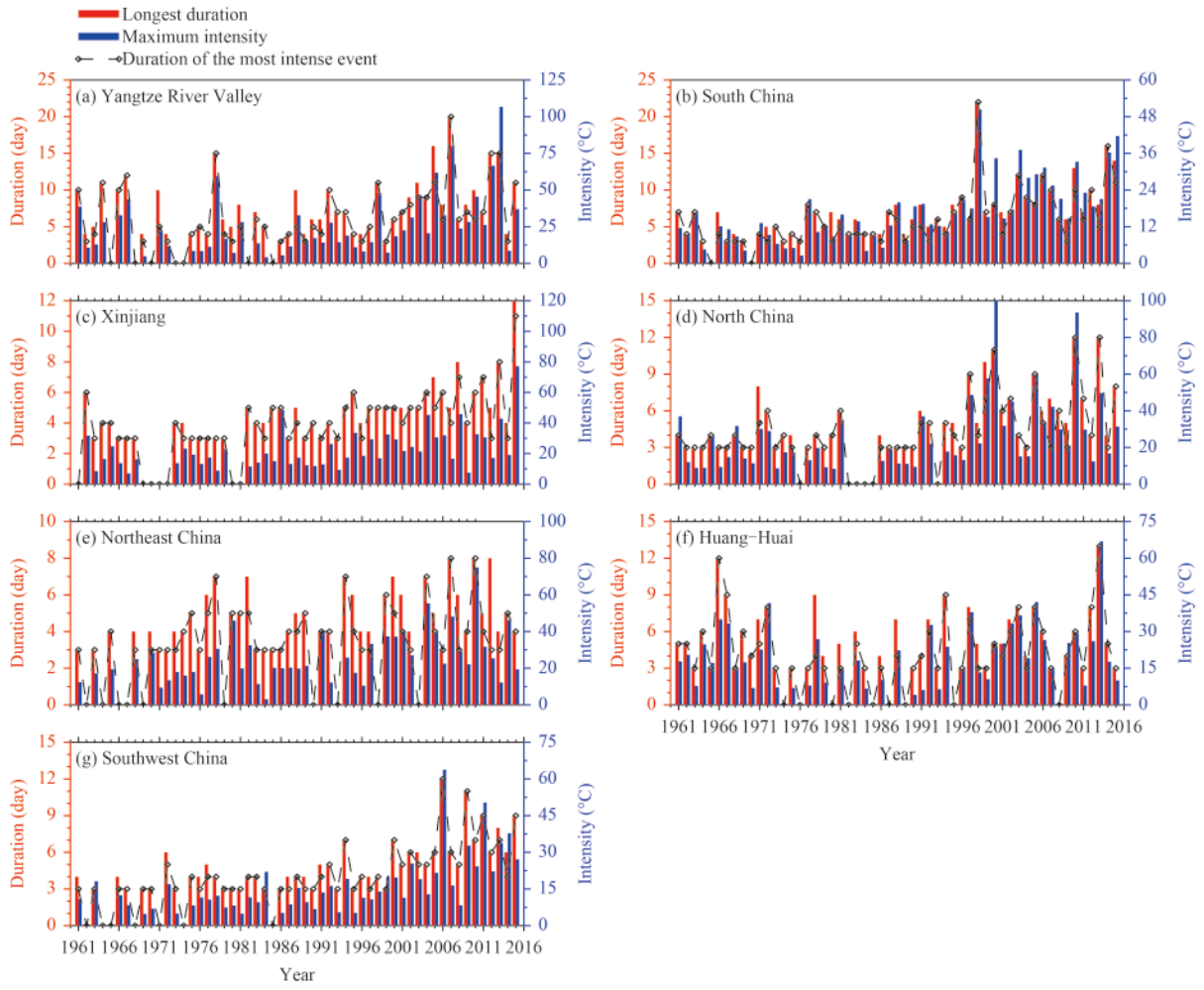

Fig. 7. Severe heat waves with longest duration (red bars and left *y*-axis) and maximum intensity (blue bars, right *y*-axis) in each sub-region. The durations for strongest events (left *y*-axis) are also illustrated by dased lines with diamonds.

non-linearly (but rather, exponentially) with duration in long-lasting HWs (Hajat et al., 2006), with an estimate of 2.5%–4% extra deaths per day beyond the first 3 HW days (Anderson and Bell, 2011). By contrast, the events with duration longer than 7 days are rarely reported in northern China, especially before 1996. In spite of the shorter duration, severe HWs in North and Northeast China are characterized by an intensity equivalent to or even greater than that of most longer-lasting HWs in the South. For example, the intensity of an 8-day event in Northeast China in 2010 (Fig. 7e) exceeded 70°C, which is greater than the intensity accumulated over 20 days in the YRV and South China. Great heat stress accumulated during a concentrated spell would swiftly damage agriculture, human thermoregulation, and local power supply. As for the events with short duration and extremely high intensity, the intensity is the ringleader of high mortality. A small rise in intensity was reportedly responsible for considerable increases in mortality in the UK and US, with an estimate of 2.47% to 4.23% of unnatural death for every extra degree above the threshold (Anderson and Bell, 2011).

What is worth noticing is that linear trends of longest duration and maximum intensity are much larger than those for mean duration and intensity (Table 1 versus Table 2). In other words, severe events have been getting even substantially severer. Consistent with variations in mean intensity and duration, increasing rate of longest duration is larger in southern China, while amplification of maximum intensity is greater in northern China. Particularly, the Yangtze River Valley, though located in southern China, has experienced greatest amplification of maximum intensity. Such an exception may be attributed to rapid urbanization and anthropogenic emissions in this region (Du et al., 2016).

Changes in the mean and variability of temperature may account for variations of HW indices (Fischer and Schär, 2010). As presented in Fig. 7, the intensity and

duration of severe HWs show marked decadal shifts, with greater duration and intensity most frequent over the last two decades. Thus, decadal variations in the mean and variability of temperature are examined via comparing probability density function (PDF) curves (Fig. 8). Increases in both mean T_{max} and T_{min} are characterized by

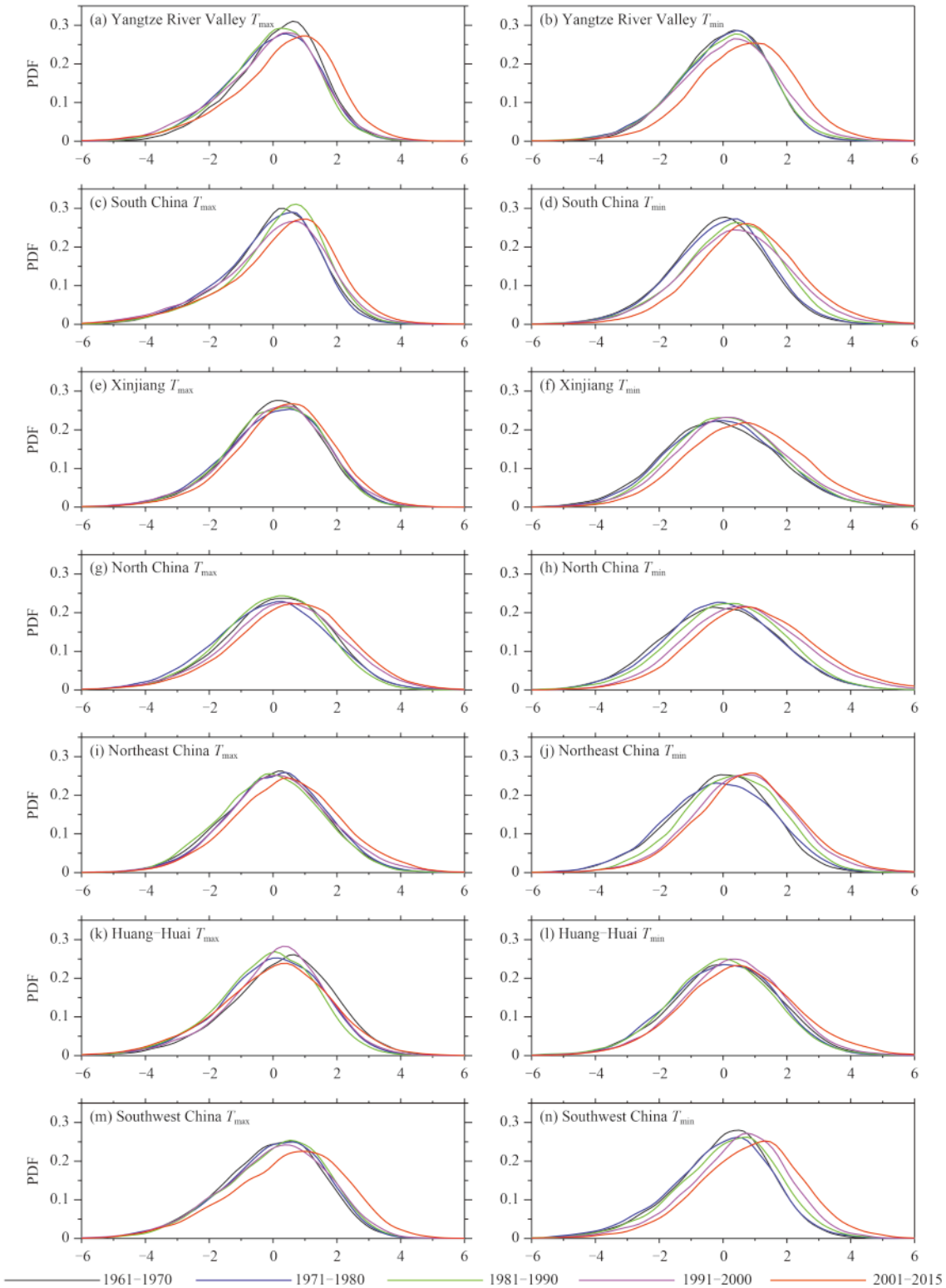

Fig. 8. Decadal changes in Probability Density Function (PDF) of T_{max} (left panels) and T_{min} (right panels) in the seven most-affected subregions whose names are indicated in the upper left of each panel.

positive shifts of PDF curves in most sub-regions, excluding the Huang–Huai region. The most obvious shift, as recorded in Southwest China, brought more hot days and nights, which has narrowed temporal gaps between isolated warm events and further lengthened HWs. This may explain why the largest increase of duration is observed in Southwest China. Generally, the shape of PDF curves in northern China is wider and flatter, indicating greater temperature variability there, notably during the last two decades. Such a variation entails more frequent appearance of excessively high T_{max}/T_{min}. These analyses imply that the recent frequent severe HWs with higher intensity in northern China are jointly contributed by increased variability and mean T_{max}/T_{min}, with the latter dominant in inducing increasing occurrences of severe HWs with longer duration and greater intensity in southern China over the past two decades.

4. Discussion and conclusions

4.1 *Limitations*

Some conclusions so far still need cautious interpreting, although a proper slope estimator (Kendall's tau) and rigorous significance tests have been applied in this study. Main estimations have been made favorably via linear trend analyses, but this approach may get stuck with HW indices possessing strong decadal oscillations, which possibly exist at stations with insignificant weak trends (Della-Marta et al., 2007). Moreover, linear trend analyses are also sensitive to the periods selected, the diversity of which may account for the differences between estimated trends in different studies. In addition to the uncertainties above, there are punchy evidence suggesting that accelerating urbanization may lead to severer HWs and hence higher mortality (Bian et al., 2015). Particularly, city expansions may raise risks of compound HWs downtown by favoring warm nights and dampened winds (Lemonsu et al., 2015). Municipal interventions and precautions should mitigate such elevated risks (Vanos et al., 2015). It is also imperative to further partition the impacts of anthropogenic activities and natural variability on heat waves (Sun et al., 2014).

The simultaneous consideration of T_{max} and T_{min} was intended to link HWs with heat-related mortality. However, few long-term mortality data are currently available for analyses in China. Very short records (usually after 2005) in limited big cities, such as Shanghai and Guangzhou, were used in previous studies (e.g., Gao et al., 2015). Long-term heat-related mortality data in other cities/stations need to be collected to support follow-up studies (Chen et al., 2015). At 19 stations located in mountains or plateaus in this study, though exceeding 90th percentile, the T_{max}/T_{min} may still be lower than 25°C/15°C, especially during early summer. At these stations, early-summer events should be more exactly referred to as "hot spells" instead of heat waves.

The PDF curves presented in Section 3.3 have qualitatively depicted decadal variation of the mean and variability of T_{max}/T_{min}. The quantitative estimation only discovered insignificant changes of kurtosis coefficients for the curves in all the sub-regions. Schär et al. (2004) revealed a nonlinear correlation between increases in temperature variability and HW intensity in Europe. Such a correlation has also been found in other regions, where very trivial and insignificant changes of kurtosis corresponded to substantial increases of HW intensity (Simolo et al., 2011).

The HW responses to global warming vary regionally. For instance, inland China's increases in HWF are similar to those in eastern America (0.5–2 days decade^{-1}, Smith et al., 2013), while the rises in duration across eastern Mediterranean region (2 days decade^{-1}, Kuglitsch et al., 2010) are much larger than those in our study. Climate model projections of compound HWs are needed to tell whether these changes of HWs will continue. A deeper understanding of HW trends may and their future behaviors could provide scientific supports for precautions against heat-related disasters.

4.2 *Conclusions*

Our study focuses on features and trends of compound HWs across China during 1961–2015. Compound HWs are defined by a combined threshold of daily maximum temperature (T_{max}) and minimum temperature (T_{min}), with both meteorological extremity and health impacts being taken into consideration. Few studies have been conducted with respect to such kind of heat waves in China.

Compound HWs are quantified by four indices, namely, HWN (number), HWF (days), HWD (duration), and HWI (intensity), whose significant increases are observed in most parts of China, except for the Huang–Huai region. The sharpest lengthening in HWD is recorded in southern China, with a maximum trend of 0.49 ± 0.18 days decade^{-1} in Southwest China. The intensity of the identified HWs rose dramatically in northern China, coastal regions along South China, and the YRV. The HWs in northern China, compared to those in southern China, are characterized by larger increases in intensity but smaller lengthening in duration. Spatial extent of HWs has expanded across China since 1961, especially in northern China. Similar increasing trends can also be

found when severe HWs with longest duration and/or maximum intensity are investigated. In terms of intensity, severe HWs in northern China could be, despite a much shorter duration, comparable to or even stronger than their counterpart in the south.

This study has provided a systematic evaluation of trends for compound heat waves in China, with an attempt to narrow the gap of understanding about such a devastating heat wave type in China and in the rest of the world.

REFERENCES

Anderson, G. B., and M. L. Bell, 2011: Heat waves in the United States: Mortality risk during heat waves and effect modification by heat wave characteristics in 43 U.S. communities. *Environmental Health Perspectives*, **119**, 210–218, doi: 10.1289/ehp.1002313.

Basu, R., and J. M. Samet, 2002: Relation between elevated ambient temperature and mortality: A review of the epidemiologic evidence. *Epidemiologic Reviews*, **24**, 190–202, doi: 10.1093/epirev/mxf007.

Bian, T., G. Y. Ren, B. X. Zhang, et al., 2015: Urbanization effect on long-term trends of extreme temperature indices at Shijiazhuang station, North China. *Theor. Appl. Climatol.*, **119**, 407–418, doi: 10.1007/s00704-014-1127-x.

Chen, K., J., Bi, J. Chen, et al., 2015: Influence of heat wave definitions to the added effect of heat waves on daily mortality in Nanjing, China. *Science of the Total Environment*, **506–507**, 18–25, doi: 10.1016/j.scitotenv.2014.10.092.

Chen, M., F. H. Geng, L. M. Ma, et al., 2013: Analyses on the heat wave events in Shanghai in recent 138 years. *Plateau Meteor.*, **32**, 597–607. (in Chinese)

Chen, Y., and P. M. Zhai, 2013: Persistent extreme precipitation events in China during 1951–2010. *Climate Research*, **57**, 143–155, doi: 10.3354/cr01171.

Della-Marta, P. M., M. R. Haylock, J. Luterbacher, et al., 2007: Doubled length of western European summer heat waves since 1880. *J. Geophys. Res.*, **112**, D15103, doi: 10.1029/2007JD008510.

Ding, T., and W. H. Qian, 2011: Geographical patterns and temporal variations of regional dry and wet heatwave events in China during 1960–2008. *Adv. Atmos. Sci.*, **28**, 322–337, doi: 10.1007/s00376-010-9236-7.

Ding, T., W. H. Qian, and Z. W. Yan, 2010: Changes in hot days and heat waves in China during 1961–2007. *Int. J. Climatol.*, **30**, 1452–1462, doi: 10.1002/joc.1989.

D'Ippoliti, D., P. Michelozzi, C. Marino, et al., 2010: The impact of heat waves on mortality in 9 European cities: Results from the EuroHEAT project. *Environmental Health*, **9**, 37, doi: 10.1186/1476-069X-9-37.

Du, H. Y., D. D. Wang, Y. Y. Wang, et al., 2016: Influences of land cover types, meteorological conditions, anthropogenic heat and urban area on surface urban heat island in the Yangtze River Delta Urban Agglomeration. *Science of the Total Environment*, **571**, 461–470, doi: 10.1016/j.scitotenv.2016.07.012.

Fischer, E. M., and C. Schär, 2010: Consistent geographical patterns of changes in high-impact European heatwaves. *Nature Geoscience*, **3**, 398–403, doi: 10.1038/ngeo866.

Gao, J. H., Y. Z. Sun, Q. Y. Liu, et al., 2015: Impact of extreme high temperature on mortality and regional level definition of heat wave: A multi-city study in China. *Science of the Total Environment*, **505**, 535–544, doi: 10.1016/j.scitotenv.2014.10.028.

García-Herrera, R., J. Díaz, R. M. Trigo, et al., 2010: A review of the European summer heat wave of 2003. *Critical Reviews in Environmental Science and Technology*, **40**, 267–306, doi: 10.1080/10643380802238137.

Grize, L., A. Huss, O. Thommen, et al., 2005: Heat wave 2003 and mortality in Switzerland. *Swiss Medical Weekly*, **135**, 200–205.

Guo, X. J., J. B. Huang, Y. Luo, et al., 2017: Projection of heat waves over China for eight different global warming targets using 12 CMIP5 models. *Theor. Appl. Climatol.*, **128**, 507–522, doi: 10.1007/s00704-015-1718-1.

Hajat, S., B. Armstrong, M. Baccini, et al., 2006: Impact of high temperatures on mortality: Is there an added heat wave effect? *Epidemiology*, **17**, 632–638, doi: 10.1097/01.ede.0000239688.70829.63.

Jiang, Z. H., J. Song, L. Li, et al., 2012: Extreme climate events in China: IPCC-AR4 model evaluation and projection. *Climatic Change*, **110**, 385–401, doi: 10.1007/s10584-011-0090-0.

Jones, P. D., S. C. B. Raper, R. S. Bradley, et al., 1986: Northern Hemisphere surface air temperature variations: 1851–1984. *J. Climate Appl. Meteor.*, **25**, 161–179, doi: 10.1175/1520-0450(1986)025<0161:NHSATV>2.0.CO;2.

Kalkstein, L. S., and K. E. Smoyer, 1993: The impact of climate change on human health: Some international implications. *Experientia*, **49**, 969–979, doi: 10.1007/BF02125644.

Kalkstein, L. S., J. S. Greene, D. M. Mills, et al., 2008: Analog European heat waves for U.S. cities to analyze impacts on heat-related mortality. *Bull. Amer. Meteor. Soc.*, **89**, 75–85, doi: 10.1175/BAMS-89-1-75.

Karl, T. R., and R. W. Knight, 1997: The 1995 Chicago heat wave: How likely is a recurrence? *Bull. Amer. Meteor. Soc.*, **78**, 1107–1119, doi: 10.1175/1520-0477(1997)078<1107:TCHWHL>2.0.CO;2.

Kuglitsch, F. G., A. Toreti, E. Xoplaki, et al., 2010: Heat wave changes in the eastern Mediterranean since 1960. *Geophys. Res. Lett.*, **37**, L04802, doi: 10.1029/2009GL041841.

Lemonsu, A., V. Viguié, M. Daniel, et al., 2015: Vulnerability to heat waves: Impact of urban expansion scenarios on urban heat island and heat stress in Paris (France). *Urban Climate*, **14**, 586–605, doi: 10.1016/j.uclim.2015.10.007.

Li, X. P., L. Wang, D. L. Chen, et al., 2013: Near-surface air temperature lapse rates in the mainland China during 1962–2011. *J. Geophys. Res.*, **118**, 7505–7515, doi: 10.1002/jgrd.50553.

Liu, J., and P. M. Zhai, 2014: Changes in climate regionalization indices in China during 1961–2010. *Adv. Atmos. Sci.*, **31**, 374–384, doi: 10.1007/s00376-013-3017-z.

Meehl, G. A., and C. Tebaldi, 2004: More intense, more frequent, and longer lasting heat waves in the 21st century. *Science*, **305**, 994–997, doi: 10.1126/science.1098704.

Patz, J. A., D. Campbell-Lendrum, T. Holloway, et al., 2005: Impact of regional climate change on human health. *Nature*,

438, 310–317, doi: 10.1038/nature04188.

Perkins, S. E., L. V. Alexander, and J. R. Nairn, 2012: Increasing frequency, intensity and duration of observed global heatwaves and warm spells. *Geophys. Res. Lett.*, **39**, L20714, doi: 10.1029/2012GL053361.

Ren, G. Y., and Y. Q. Zhou, 2014: Urbanization effect on trends of extreme temperature indices of national stations over mainland China, 1961–2008. *J. Climate*, **27**, 2340–2360, doi: 10.1175/JCLI-D-13-00393.1.

Robinson, P. J., 2001: On the definition of a heat wave. *J. Appl. Meteor.*, **40**, 762–775, doi: 10.1175/1520-0450(2001)040<0762:OTDOAH>2.0.CO;2.

Schär, C., P. L. Vidale, D. Lüthi, et al., 2004: The role of increasing temperature variability in European summer heat waves. *Nature*, **427**, 332–336, doi: 10.1038/nature02300.

Sen, P. K., 1968: Estimates of the regression coefficient based on Kendall's tau. *Journal of the American Statistical Association*, **63**, 1379–1389, doi: 10.1080/01621459.1968.10480934.

Serreze, M. C., J. E. Walsh, F. S. Chapin III, et al., 2000: Observational evidence of recent change in the northern high-latitude environment. *Climatic Change*, **46**, 159–207, doi: 10.1023/A:1005504031923.

Simolo, C., M. Brunetti, M. Maugeri, et al., 2011: Evolution of extreme temperatures in a warming climate. *Geophys. Res. Lett.*, **38**, L16701, doi: 10.1029/2011GL048437.

Smith, T. T., B. F. Zaitchik, and J. M. Gohlke, 2013: Heat waves in the United States: Definitions, patterns and trends. *Climatic Change*, **118**, 811–825, doi: 10.1007/s10584-012-0659-2.

Stocker, T. F., D. Qin, G. K. Plattner, et al., 2013: *Climate Change* 2013: *The Physical Science Basis. Contribution of Working Group I to the Fifth Assessment Report of the Intergovernmental Panel on Climate Change*. Cambridge University Press, 1308 pp.

Sun, Y., X. B. Zhang, F. W. Zwiers, et al., 2014: Rapid increase in the risk of extreme summer heat in Eastern China. *Nature Climate Change*, **4**, 1082–1085, doi: 10.1038/nclimate2410.

Vanos, J. K., L. S. Kalkstein, and T. J. Sanford, 2015: Detecting synoptic warming trends across the US Midwest and implications to human health and heat-related mortality. *Int. J. Climatol.*, **35**, 85–96, doi: 10.1002/joc.3964.

Wang, L. Y., X. Yuan, Z. H. Xie, et al., 2016: Increasing flash droughts over China during the recent global warming hiatus. *Scientific Reports*, **6**, 30571, doi: 10.1038/srep30571.

Wang, Z. Y., Y. H. Ding, Q. Zhang, Y. F. Song, et al., 2012: Changing trends of daily temperature extremes with different intensities in China. *Acta Meteor. Sinica*, **26**, 399–409, doi: 10.1007/s13351-012-0401-z.

Wei, K., and W. Chen, 2011: An abrupt increase in the summer high temperature extreme days across China in the mid-1990s. *Adv. Atmos. Sci.*, **28**, 1023–1029, doi: 10.1007/s00376-010-0080-6.

Xia, J. J., K. Tu, Z. W. Yan, et al., 2016: The super-heat wave in eastern China during July–August 2013: A perspective of climate change. *Int. J. Climatol.*, **36**, 1291–1298, doi: 10.1002/joc.2016.36.issue-3.

Xue, Y. K., 1996: The impact of desertification in the Mongolian and the Inner Mongolian grassland on the regional climate. *J. Climate*, **9**, 2173–2189, doi: 10.1175/1520-0442(1996)009<2173:TIODIT>2.0.CO;2.

Ye, D. X., J. Yin, Z. H. Chen, et al., 2013: Spatiotemporal change characteristics of summer heatwaves in China in 1961–2010. *Progressus Inquisitiones de Mutatione Climatis*, **9**, 15–20, doi: 10.3969/j.issn.1673-1719.2013.01.003. (in Chinese)

Zhang, X. B., L. Alexander, G. C. Hegerl, et al., 2011: Indices for monitoring changes in extremes based on daily temperature and precipitation data. *Wiley Interdisciplinary Reviews: Climate Change*, **2**, 851–870, doi: 10.1002/wcc.147.

Zou, X. K., P. M. Zhai, and Q. Zhang, 2005: Variations in droughts over China: 1951–2003. *Geophys. Res. Lett.*, **32**, doi: 10.1029/2004GL021853.

Tech & Copy Editor: Lan YI
Language Editor: Lan YI